

A phase reconstruction algorithm for Lamb wave based structural health monitoring of anisotropic multilayered composite plates

Jagannathan Rajagopalan,^{a)} Krishnan Balasubramaniam, and C. V. Krishnamurthy
Center for Nondestructive Evaluation and Department of Mechanical Engineering,
Indian Institute of Technology Madras, Chennai-600036, India

(Received 4 May 2005; accepted 11 November 2005)

Platelike structures, made of composites, are being increasingly used for fabricating aircraft wings and other aircraft substructures. Continuous monitoring of the health of these structures would aid the reliable operation of aircrafts. This paper considers the use of a Lamb wave based structural health monitoring (SHM) system to identify and locate defects in large multilayered composite plates. The SHM system comprises of a single transmitter and multiple receivers, coupled to one side of the plate that send and receive Lamb waves. The proposed algorithm processes the data collected from the receivers and generates a reconstructed image of the material state of the composite plate. The algorithm is based on phased addition in the frequency domain to compensate for the dispersion of Lamb waves. In addition, small deviations from circularity of the slowness curves of Lamb wave modes, due to anisotropy, are corrected for by assuming that the phase and group velocity directions coincide locally. Experiments were performed on an anisotropic multilayered composite plate containing a single defect. Reconstruction of the defect is carried out using data for a weakly anisotropic Lamb wave mode as a proof of concept of the proposed algorithm. © 2006 Acoustical Society of America. [DOI: 10.1121/1.2149775]

PACS number(s): 43.35.Zc, 43.35.Cg, 43.60.Fg [YHB]

Pages: 872–878

I. INTRODUCTION

Multilayered composites, in the form of platelike structures, are being increasingly used in variety of structures because of the unique properties they offer. In particular, they are often used for fabricating wings and other substructures of aircrafts. Inspection of these large structures using traditional nondestructive evaluation methods is both time consuming and difficult, especially if the monitoring has to be done *in situ*. Lamb wave based inspection methods have been shown to be well suited for monitoring such structures, since Lamb waves have the capability of traveling large distances without much attenuation. But, Lamb waves are dispersive in nature and hence the velocity of propagation becomes a function of the wave frequency, the thickness of the plate, and the direction of travel (in case the medium is anisotropic). Hence, analyzing Lamb wave data to evaluate the integrity of structures becomes complicated.

Moreover, most of the classical theoretical work on Lamb waves is based on assuming the wave vectors to be one-dimensional.¹ But, in practice the wave vectors need to be two-dimensional. This is because for effective structural health monitoring, it is desirable that the wave interrogates the material at different angles. Also, reflections from a structural feature in the plate may propagate along any direction in the plane of the plate. Hence, it is necessary to incorporate directionality in any inspection procedure in order to image damage in composite materials. The suitability of an

array based approach for achieving directionality has been demonstrated in Refs. 2 and 3. The applicability of an array based system for rapid inspection of isotropic plate structures was demonstrated in Refs. 4 and 5, wherein beam steering algorithms were used to process data collected from omnidirectional guided wave transducer arrays. Structural health monitoring of isotropic and anisotropic platelike structures by processing data from multiple transmitters and multiple receivers (MTMR) using tomographic reconstruction techniques has been reported elsewhere.^{6–8}

In this paper, we seek to extend the flaw detection technique demonstrated for isotropic plate-like structures in Refs. 4 and 5 to anisotropic materials. In anisotropic plates, such as the fiber reinforced composite laminates, the energy propagation direction is along the preferred “group” velocity direction and can be determined through the analysis of the slowness surface (inverse of velocity profile).^{9–14} Anisotropy in solid materials has a tendency to change the direction of the energy of the acoustic wave propagation along preferred orientations. The energy propagation direction at any “phase” velocity angle (wave vector direction) is oriented along the normal to the slowness surface measured at that “phase” angle. Hence, any algorithm for Lamb wave reconstruction in anisotropic materials, unlike in isotropic materials, must consider this dependency of the phase velocity and energy on the direction of wave travel.

The first part of this paper deals with the description of the array system and the method of data acquisition. The second part describes the algorithm for material state reconstruction in anisotropic materials. The final part shows the results of applying the algorithm to experimental data. For

^{a)}Presently at the Department of Mechanical and Industrial Engineering, University of Illinois Urbana-Champaign.

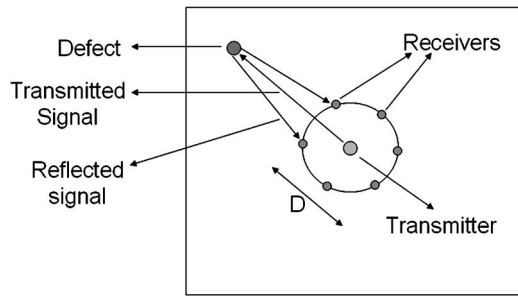


FIG. 1. Architecture for the Lamb wave based SHM system.

applying the algorithm, the dispersion characteristics of the anisotropic material for wave propagation along all directions need to be known *a priori*.

II. ARRAY DESCRIPTION AND DATA ACQUISITION

As indicated in Fig. 1, the array consists of a single transmitter and N number of receivers coupled to one surface of the plate. The receivers are arranged in a circle of diameter D while the transmitter is placed at the center. A polar coordinate system is defined with its origin at the center of the array coinciding with the transmitter position. The positions of the receivers are defined using their radial and angular coordinates. It is assumed that the transmitter and the receivers act as point sources and have equal transmission and reception sensitivity in all directions.

The data acquisition and transformation process begins with the acquisition of the raw data set in the time, \mathbf{t} , domain. The transmitter is excited and a discretely sampled \mathbf{t} domain signal is collected at each of the receivers. This data is used to form a matrix, \mathbf{T} , in which each column represents the raw \mathbf{t} domain signal collected at each of the N receivers. Consequently, the number of columns in the \mathbf{T} matrix is equal to the number of receivers. A column wise fast Fourier transform (FFT) is, then, performed on the \mathbf{T} matrix to transform it to a matrix, \mathbf{F} , containing the complex spectra in the frequency, ω , domain. The transformation to the frequency domain is done so that the effects of guided wave dispersion can be taken into account.

III. PHASE RECONSTRUCTION ALGORITHM

The purpose of the phase reconstruction algorithm is to determine the locations from which the waves sent by the transmitter are reflected back. In the algorithm, the reflected wave packets are assumed to come from a particular direction (angle) and the signal received at each receiver is shifted appropriately (in the ω domain) and added. If the assumed direction is the actual direction of the reflected wave then this process results in a coherent addition. This procedure is repeated for a set of equi-spaced angles that span the entire 360° . The phase-reconstructed signals are then transformed into the wave number domain, \mathbf{k} , using interpolation. The locations from which the waves are reflected back are then obtained by performing an IFFT on these phase-reconstructed signals.

As mentioned earlier, algorithms for beam steering from omni-directional transducer arrays, using phased addition in

the \mathbf{k} domain have been proposed in Refs. 4 and 5. But such algorithms are restricted to isotropic materials where a transformation from \mathbf{t} domain to ω domain and subsequently to \mathbf{k} domain is possible. In anisotropic materials, the wave number is a function of both the wave frequency and the direction of wave propagation. Hence, a transformation from the \mathbf{t} domain to \mathbf{k} domain is not possible when the direction of wave propagation is not known, as is the case with reflections from unknown defects.

In the first step of the algorithm, a particular guided wave mode is chosen and phased addition of the columns of the \mathbf{F} matrix is performed along n equispaced reconstruction angles using the dispersion characteristics of the mode. These reconstruction angles, represented by θ_p , are the assumed angles of propagation of the reflected waves. This phased addition in the ω domain leads to a matrix, \mathbf{Q} , in which the rows represent different frequencies, ω_k , and the columns represent different reconstruction angles, θ_p . The elements in \mathbf{Q} are calculated using the following expression:

$$Q_{\omega p} = \sum_{j=1}^N f_{\omega j} \exp(-i2\pi k(\omega_k, \theta_p)x_{pj}), \quad (1)$$

where

$$x_{pj} = R_j \cos(\Phi_j - \theta_p). \quad (2)$$

In the above expressions R_j and Φ_j are the polar coordinates of the j th receiver, while x_{pj} represents the change in path length required for the signal received at the j th receiver to maintain coherence along θ_p .

In making the phase corrections to $f_{\omega j}$'s in Eq. (1), the algorithm assumes that the phase velocity and group velocity directions are the same locally. For the spatially tight transmit-receive configuration considered, and for a flaw in the far-field where the algorithm is intended to be applied, the ray paths from the transmitter to the flaw and from the flaw to the receivers can be taken to be nearly equal along the given orientation based on the principle of reciprocity. Accordingly, the algorithm is expected to be applicable for weakly anisotropic materials over all angles, for moderate anisotropic materials over angular sectors around symmetry axes and for strongly anisotropic materials along the symmetry axes. For the algorithm to be applicable even for strongly anisotropic materials, one has to first obtain the phase velocity angle, Ψ_p , corresponding to the group velocity angle θ_p and then use $k(\omega_k, \Psi_p)$ for making the phase correction.

Proceeding to the next step of the algorithm, the dispersion characteristics of the chosen guided wave mode are used for the different directions, θ_p , and each column in \mathbf{Q} is separately interpolated to obtain a matrix, \mathbf{W} , where each column contains spectra at points equispaced in the \mathbf{k} domain. The interpolation procedure for single column is performed as follows. Let $\omega_1, \omega_2, \dots, \omega_m$ be the m discrete equispaced frequencies corresponding to the m rows in \mathbf{Q} , with ω_1 as the minimum frequency and ω_m as the maximum. For a particular column, representing a particular angle, let k_1, k_2, \dots, k_m be the wave numbers corresponding to the guided wave mode of interest (k_1, k_2, \dots, k_m are known since both the frequency and the angle of wave propagation are known).

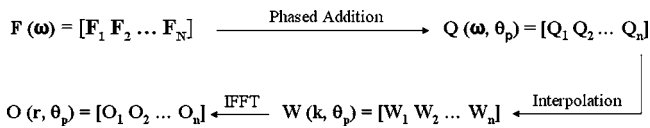


FIG. 2. Phase reconstruction and inversion procedure for Lamb waves in anisotropic materials.

Hence, the spectra at k_1, k_2, \dots, k_m is known. But, the wave numbers k_1, k_2, \dots, k_m are not equispaced since the phase velocity changes with frequency. Hence, m equispaced wave numbers, k'_1, k'_2, \dots, k'_m , are chosen between k_1 and k_m with $k'_1 (=k_1)$ as the minimum and $k'_m (=k_m)$ as the maximum. Since the spectra at k_1, k_2, \dots, k_m is known, the spectra at k'_1, k'_2, \dots, k'_m can be obtained by interpolation.

To obtain the output matrix, \mathbf{O} , in the polar domain, the columns in \mathbf{W} are subject to an inverse fast Fourier transform (IFFT) to convert them from the \mathbf{k} - θ domain to the \mathbf{r} - θ domain. Now each element in \mathbf{O} has a corresponding radial and angular position attached to it. Reconstruction is obtained by plotting the amplitudes of the elements in \mathbf{O} as a function of their polar position. The procedure for phase reconstruction is summed up in Fig. 2.

The effectiveness of this algorithm for imaging the flaw in the “near field” is limited by the assumption made during the phase reconstruction. Here, the “near field” is defined to be approximately 2–3 times the diameter of the sensor configuration (D). The phase correction algorithm effectively approximates the path lengths between the flaw and the receiver to be equal to the projection along the angle that is being reconstructed.^{4,5} While this assumption is valid in the “far field,” this approximation does lead to distortions in the flaw imaging in the “near field” region.

Also, it must be noted that as the sensor configuration diameter D increases, the phase resolution in the “far field” increases leading to improved reconstruction. However, the increase in D will result in an increase in the “near field” region. Hence, the diameter D is a critical parameter that must be carefully chosen depending on the type of structure and the region of critical flaw location.

IV. EXPERIMENTS AND RESULTS

Two experiments, the first to reconstruct the edges of a composite plate, and the second to reconstruct a defect (hole) in the composite plate, were performed to validate the algorithm. The plate, 3.15 mm thick, was made of 21 layers of unidirectional composite, each 0.15 mm thick. The fiber orientation in the first 7 layers was as follows: $+45^\circ, -45^\circ, 0^\circ, 90^\circ, 0^\circ, -45^\circ$, and $+45^\circ$. The same pattern was repeated in the next 14 layers. To obtain the dispersion curves, the averaged properties of the material were used. Using the engineering constants of the unidirectional composite, the elastic coefficients were found and the elastic coefficients matrix was formed. Then the effective elastic coefficients matrix for different orientations ($+45^\circ, -45^\circ, 90^\circ$) was found by transforming the elastic coefficient matrix in the respective direction. The elastic coefficients matrix for each orientation was then multiplied by the number of layers (since each layer is of same thickness) in that particular orientation and added

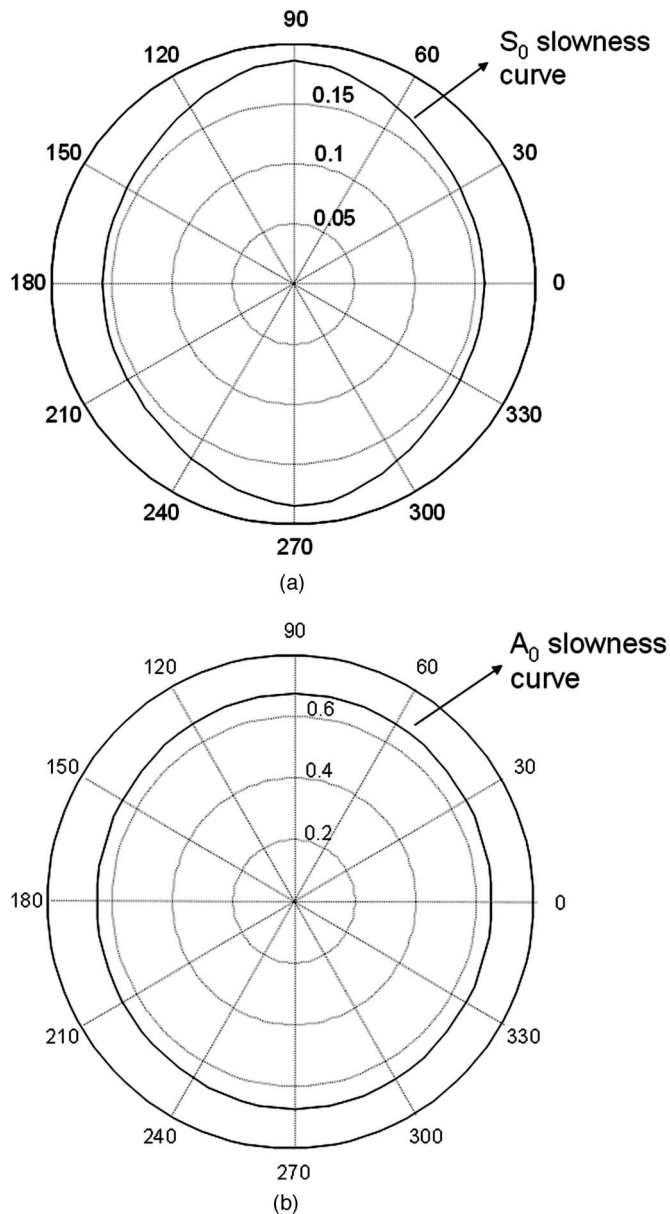


FIG. 3. Slowness curves of (a) S_0 mode and (b) A_0 mode for 3.15 mm thick multilayered composite plate.

together. This matrix was divided by the total number of layers to get the “effective” elastic coefficients matrix.^{15,16} The “effective” elastic coefficients matrix was used to obtain the dispersion curves in different directions using the DISPERSE™ software (developed by Imperial College, UK). Typical slowness curves for S_0 mode, used in the reconstructions, and A_0 mode are shown in Figs. 3(a) and 3(b), respectively. As can be seen from the figures, the slowness profile of the S_0 mode shows a fair amount of variation with angle while that of the A_0 mode is relatively uniform. The radii of the circles in Fig. 3 are in ms/m.

In both the experiments, a Panametrics 5058PR broadband Pulser/Receiver was used to excite a Panametrics Videoscanner 500 kHz Transducer, which was used as a transmitter. A similar transducer was used as receiver. An Agilent 54621A oscilloscope was used for signal acquisition. The receiver was kept at 18 equispaced locations on a circle, of

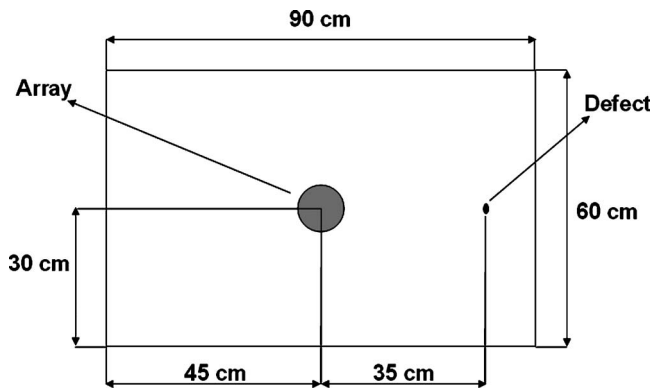


FIG. 4. Plate dimensions, array, and defect locations for the experiments.

10 cm diameter with the transmitter at the center, and signals were collected at each of these locations to simulate an array with 18 receivers. The transmitter was excited with a 100 V signal with center frequency of 500 kHz. The signals were sampled at 2.5 MHz and filtered after acquisition using a band pass filter of 100–1000 kHz range to eliminate noise and undesirable low frequency components. The dimensions of the plate and locations of the array and the defect (for the second experiment) are shown in Fig. 4.

Figure 5 shows the reconstruction after applying the algorithm, with 36 reconstruction angles. The gray scale on the plot is logarithmic with a range of 12 decibel (dB). The array is marked at the center and the edges can be seen at the appropriate locations as black patches, the black patches indicating higher amplitudes obtained as a result of the coherent addition of the reflected signals obtained at the various receivers. When the dB range of the reconstruction is increased, a few artifacts show up. Figure 6 shows the reconstruction with the same experimental data, assuming the plate to be isotropic, with the dispersion characteristics for $\theta=0^\circ$ propagation being used as the dispersion characteristics for all directions. In this reconstruction, only the edges along $\theta=0^\circ$ and $\theta=180^\circ$ are located accurately, indicating the need to incorporate the anisotropic correction during reconstruction.

A typical waveform obtained at a receiver, comprising both the transmitted and reflected signals, is shown in Fig. 7.

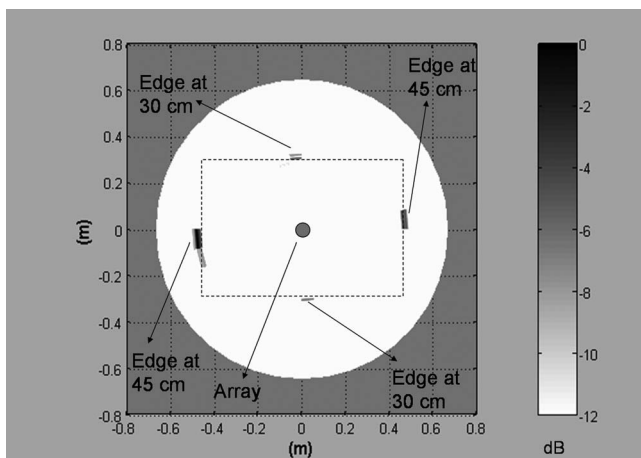


FIG. 5. Reconstruction of edges of composite plate with 12 dB range.

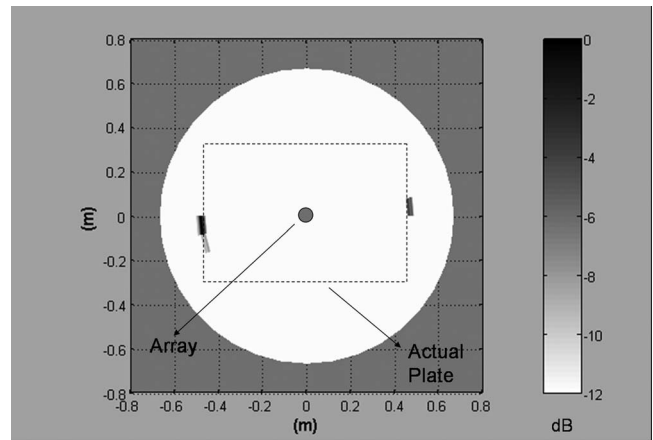


FIG. 6. Reconstruction of edges, assuming the plate to be isotropic, with the dispersion characteristics for $\theta=0^\circ$ being used as the dispersion characteristics for all directions.

Figures 8(a) and 8(b) show the frequency content of the transmitted and reflected signals. While the transmitted signal has a large frequency content around the excitation frequency at 500 kHz, the reflected signals have most of their frequency content around 200 kHz. Since only the S_0 and A_0 modes exist at these frequencies and S_0 is the faster among them and did not show much attenuation, it was chosen for reconstruction. Another reason for using S_0 was that it seemed to undergo no mode conversion at the edges. We suspect that the frequencies around 500 kHz in the transmitted signal get attenuated because the dominant S_0 mode is highly dispersive around that frequency.

In the second experiment a roughly oval-shaped hole, 0.4 cm wide and 0.8 cm long, was drilled in the 0° direction at a distance of 35 cm from the center of the plate (Fig. 4), to induce a defect in the plate. The flaw was chosen to simulate a through hole that can occur due to high energy impacts on aircraft wings, or even moderate impacts, if they occurred at locations that already had some internal defect, like a void. As the technique is intended for locating damage in large plates, the edge-effects arising out of using a small plate had to be kept to a minimum. The flaw location was chosen such that the interference to the signal reflected from the flaw

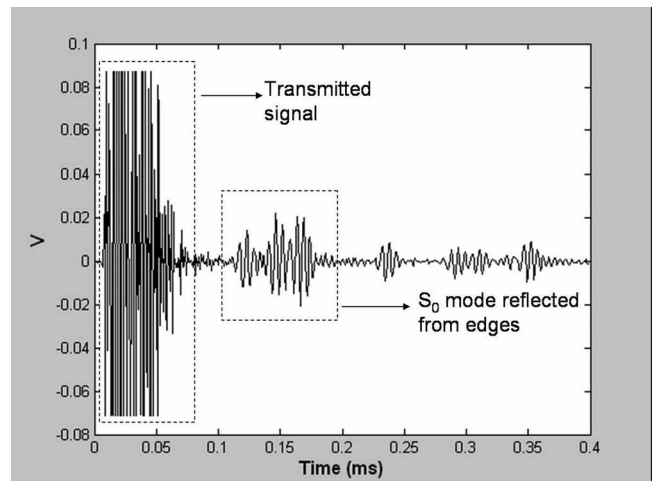
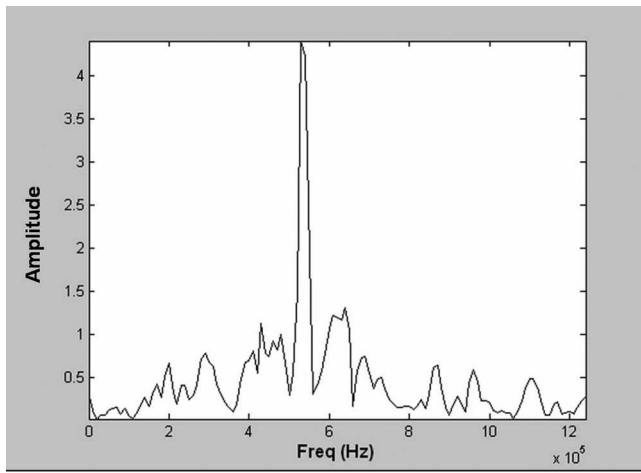
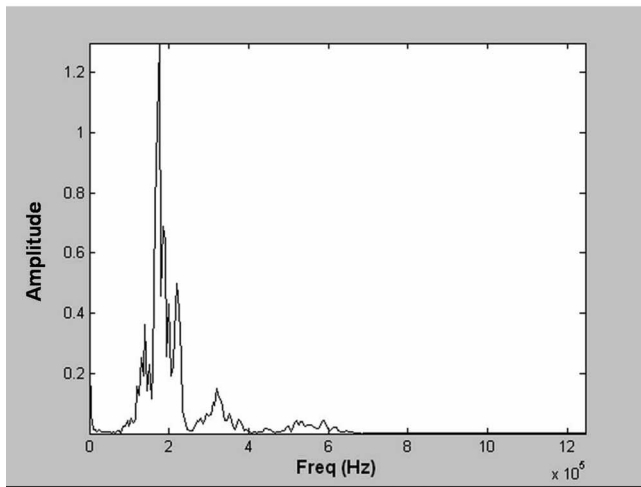


FIG. 7. A typical waveform obtained at a receiver.



(a)



(b)

FIG. 8. Frequency contents of (a) transmitted signal and (b) reflected signal.

from edge and corner reflections as well as the transmitted signal was minimal. The distance of the flaw from the array was chosen such that it was sufficiently far off to avoid any “near field” effects. The data was collected in the same manner as in the first experiment. Figure 9 shows the reconstruction

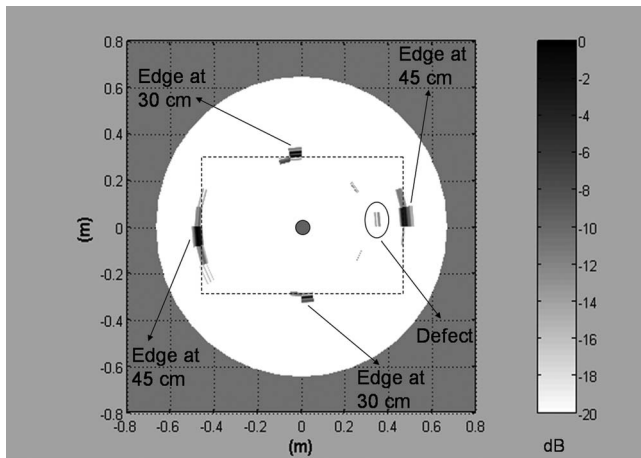


FIG. 9. Reconstruction of defect (hole) in the composite plate with 20 dB range.

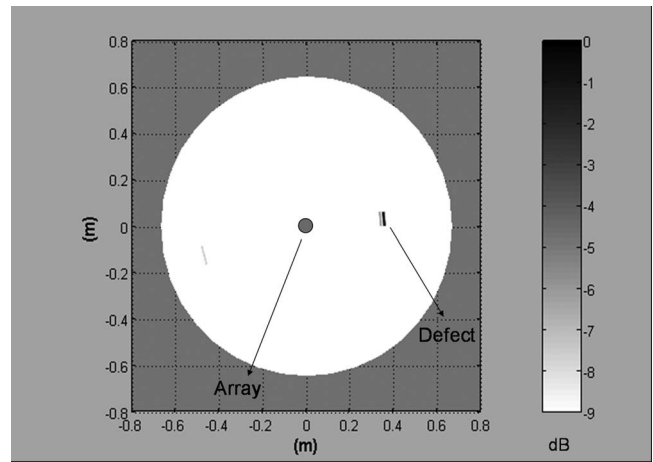


FIG. 10. Reconstruction of defect using difference of amplitudes, with 9 dB range.

tion with a range of 20 dB, the reconstruction being presented with a higher dB range so that the defect can be seen more clearly.

While the presence of the defect can be made out in Fig. 9, the clarity is not very good since the reflection from the edges dominate over the reflection from the defect. Therefore, to get a better reconstruction, the output matrix \mathbf{O} (containing the amplitude at different locations) obtained from the first experiment (when the plate was defect less) was subtracted from the output matrix \mathbf{O} of the second experiment and the difference was plotted in the logarithmic scale. This was done so that the reflection from the edges cancelled out leaving only the reflection from the defect. Figures 10 and 11 show the logarithmic plot of the difference of the \mathbf{O} matrices, \mathbf{O}' , with 9 dB and 12 dB range, respectively. A comparison of Figs. 9 and 10 reveals that the use of \mathbf{O}' as a reconstruction parameter does indeed leads to the suppression of the edge reflections to a very good extent, though it must be noted that Fig. 10 has a lower dB scale. But, even if the plot is on a 12 dB scale (which has been used throughout), as in Fig. 11, the edge reflections are much weaker as a comparison with Fig. 5 would readily reveal. If the reconstruction is plotted with even higher dB ranges, a few other artifacts, mainly due to noise in the signals, do show up. Hence, a calibration procedure may be necessary in order to reduce the number of false alarms during SHM. All the reconstructions for the second experiment were obtained with 36 reconstruction angles.

The analytical method for obtaining the dispersion curves can be used if the material properties and the ply lay-up for the composite are available. Alternatively, if such information is not available, the single-transmitter-multiple-receivers (STMR) array allows for a self-calibration mode for obtaining the dispersion function, since the receivers first receive the transmitted wave. In the self-calibration mode, the anisotropy and the dispersion properties, as function of orientation, can be experimentally derived from the first received signal at each of the receivers. The wave velocities of the individual modes can be obtained by measuring the time difference between the trigger and the arrival time of the received signal at each of the receiver. If sufficient numbers

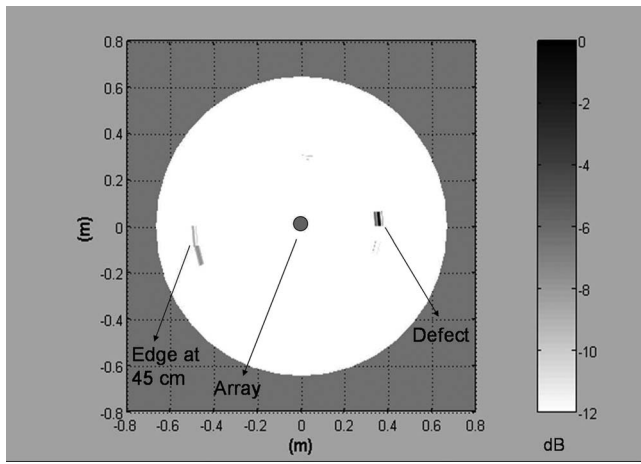


FIG. 11. Reconstruction of defect using difference of amplitudes, with 12 dB range.

of velocity are available, the elastic moduli that define the wave propagation can be obtained by using inverse techniques that have been documented.^{17–20} Once the elastic moduli are obtained, the dispersion curve for the fundamental modes can be computed. Another technique for obtaining the dispersion behavior of the as received Lamb wave mode would be to utilize the time-frequency transforms such as wavelets.^{21,22} Once the dispersion characteristics, as a function of orientation, have been experimentally obtained using the self-referencing mode, they can be then used in the phase reconstruction algorithm in the SHM mode. However, for this to be reliable the number of receivers must be sufficiently high.

V. SUMMARY

In this paper, a method for structural health monitoring (SHM) of anisotropic platelike structures using a STMR array of transducers has been developed. The method uses a new phase reconstruction algorithm, which takes into account the directional dependence of the Lamb wave dispersion characteristics in anisotropic plates, for processing data obtained from the STMR array. A system which is conceptually similar to the STMR array, but using only a single PZT transmitter and receiver, has been shown to be capable of locating damage of dimensions much smaller than the plate dimension with good accuracy. The phase reconstruction algorithm works well in the “far field,” but may show distortions/artifacts in the “near field” which is the region within approximately 2–3 times the sensor configuration diameter (D). Also, more experiments, with different flaws, need to be performed to assess the efficacy of this technique to image other types of defects.

It has been demonstrated elsewhere⁵ that a multiple-transmitter-multiple-receiver array system provides a better signal to noise ratio, which results in images with improved resolution and clarity for plates made from isotropic materials. But a STMR system was chosen here since it requires simpler electronics and a reduced footprint (desired during the SHM of aerospace structures). Also, other types of piezomaterials like PVDF film sensors (which have good recep-

tion capabilities but poor transduction capabilities) can be used as receivers in an STMR system along with a PZT transmitter. Other options include MEMS and Fiber Optics based sensor systems. This will result in a much lighter and a more compact array system.

Several other array based inspection techniques have been used by researchers to increase the signal to noise ratio so that better quality images of the damage location can be obtained. Two such techniques are based on beam forming using “phased arrays” and time-reversal concepts, demonstrated for example in Refs. 23 and 24, respectively. However, for the time-reversal concept, several issues, like accounting for group velocity change with direction, still needs to be resolved. Another technique used to identify damage in platelike structures has been by measuring changes in its dynamic response to external excitations.²⁵ An ultrasonic pulse is sent through the structure and an array of sensors is used to measure some physical parameter like displacement, velocity, etc., at selected points. The physical quantity measured by the sensors changes if the structure suffers any damage and this change can be used to identify and locate the damage. While this technique offers the advantage of a fairly sparse sensor configuration, it does not provide accurate localization of the damage. The success of this technique also depends to some extent on selecting the right parameter.

The technique demonstrated in this paper to image features in the structure, such as voids and/or delaminations, that reflect guided waves back to several or all the receivers, offers good localization of the defect, has a compact and small footprint for the sensor configuration, is easy to implement, and is applicable to anisotropic materials. For anisotropic materials which are not well characterized, i.e., the elastic properties and ply orientations are not available *a priori*; the STMR array can be designed to be self-calibrating by using the initial signal received by the receivers to measure the velocity and energy distribution profiles. These profiles lead to the evaluation of the dispersion relationships that can subsequently be employed for the phase reconstruction algorithm. STMR configurations, other than the circular configuration considered here, can be tailored to account for the anisotropy of the material, to improve the SHM of composite structures.

ACKNOWLEDGMENTS

This work was funded by the Aeronautical Development Agency, Bangalore through the DISMAS program.

¹I. Victorov, *Rayleigh and Lamb Waves: Physical Theory and Applications* (Plenum, New York, 1967).

²R. Sicard, J. Goyette, and D. Zellouf, “A SAFT algorithm for Lamb wave imaging of isotropic platelike structures,” *Ultrasonics* **39**, 487–494 (2002).

³P. Wilcox, M. Lowe, and P. Cawley, “Lamb and SH wave transducer arrays for the inspection of large areas of thick plates,” in *Review of Progress in Quantitative Nondestructive Evaluation* (American Institute of Physics, Melville, New York, 1999), Vol. 19A, pp. 1049–1056.

- ⁴P. D. Wilcox, "Guided wave beam steering from omnidirectional transducer arrays," in *Review of Progress in Quantitative Nondestructive Evaluation* (American Institute of Physics, Melville, New York, 2002), Vol. 22A, pp. 761–768.
- ⁵P. D. Wilcox, "Omnidirectional guided wave transducer arrays for the rapid inspection of large areas of plate structures," *IEEE Trans. Ultrason. Ferroelectr. Freq. Control* **50**(6), 699–709 (2003).
- ⁶S. Mahadev Prasad, R. Jagannathan, Krishnan Balasubramaniam, and C. V. Krishnamurthy, "Structural health monitoring of anisotropic layered composite plates using guided ultrasonic Lamb wave data," in *Review of Progress in Quantitative Nondestructive Evaluation* (American Institute of Physics, Melville, New York, 2003), Vol. 23B, pp. 1460–1467.
- ⁷S. Mahadev Prasad, Krishnan Balasubramaniam, and C. V. Krishnamurthy, "Structural health monitoring of composite structures using Lamb wave tomography," *Smart Mater. Struct.* **13**, N73–N79 (2004).
- ⁸R. Jagannathan, B. V. Somasekhar, Krishnan Balasubramaniam, and C. V. Krishnamurthy, "Plate waves structural health monitoring of composite structures," *Review of Progress in Quantitative Nondestructive Evaluation* (American Institute of Physics, Melville, New York, 2005), Vol. 24B, pp. 1802–1808.
- ⁹A. H. Nayfeh, *Wave Propagation in Layered Anisotropic Media* (North-Holland, Amsterdam, 1995).
- ¹⁰B. A. Auld, *Acoustic Fields and Waves in Solids*, 2nd ed. (Krieger, Malabar, 1990), Vols. 1 and 2.
- ¹¹R. Sullivan, K. Balasubramaniam, and A. G. Bennett, "Plate wave flow patterns for ply orientation imaging in fiber reinforced composites," *Mater. Eval.* **54**(4), 518–523 (1996).
- ¹²K. Balasubramaniam and Y. Ji, "Guided wave analysis in inhomogeneous plates," in *Review of Progress in Quantitative Nondestructive Evaluation* (American Institute of Physics, Melville, New York, 1995), Vol. 14, pp. 227–234.
- ¹³K. Balasubramaniam and Y. Ji, "Influence of skewing on the acoustic wave energy vector behavior in anisotropic material systems," *J. Synchrotron Radiat.* **236**(1), 166–175 (2000).
- ¹⁴S. Baly, C. Potel, J.-P. de Belleval, and M. Lowe, "Numerical and experimental deviation of monochromatic Lamb wave beam for anisotropic multilayered media," *Review of Progress in Quantitative Nondestructive Evaluation*, edited by D. O. Thompson and D. E. Chimenti, AIP Proceedings, CP615, Vol. 21, 270–278 (2002).
- ¹⁵T. D. Lhermitte and B. Perrin, "Anisotropy of the elastic properties of cross-ply fiber-reinforced composite materials," *Proc.-IEEE Ultrason. Symp.*, pp. 825–830 (1991).
- ¹⁶John J. Ditri and Joseph L. Rose, "An experimental study on the use of static effective modulus theories in dynamic problems," *J. Compos. Mater.* **27**(9), 934–943 (1993).
- ¹⁷R. A. Kline, *Nondestructive Characterization of Composite Media* (Technomic, Lancaster, 1992).
- ¹⁸J. J. Ditri, "On the determination of the elastic moduli of anisotropic media from limited acoustical data," *J. Acoust. Soc. Am.* **95**(4), 1761–1767 (1994).
- ¹⁹K. Balasubramaniam and N. S. Rao, "Inversion of composite material elastic constants from ultrasonic bulk wave phase velocity data using genetic algorithms," *Composites, Part B* **29**(B), 171–180 (1998).
- ²⁰K. Balasubramaniam, "Inversion of ply lay-up sequence for multi-layered fiber reinforced composite plates using a genetic algorithm," *Nondestruct. Test. Eval.* **15**, 311–331 (1999).
- ²¹K. L. Veroy, S. C. Wooh, and Y. Shi, "Analysis of dispersive waves using wavelet transform," in *Review of Progress in Quantitative Nondestructive Evaluation* (American Institute of Physics, Melville, New York, 1999), Vol. 18, pp. 687–694.
- ²²M. Niethammer, L. J. Jacobs, J. Qu, and J. Jayrzynski, "Time frequency representation of Lamb waves using reassigned spectrogram," *J. Acoust. Soc. Am.* **107**, L19–L24 (2000).
- ²³Shankar Sundararaman, Douglas E. Adams, and Elias J. Rigas, "Structural damage identification in homogeneous and heterogeneous structures using beamforming," *Structural Health Monitoring: An International Journal* **4**(2), 171–190 (2005).
- ²⁴Chun H. Wang, James T. Rose, and Fu-Kuo Chang, "A synthetic time-reversal imaging method for structural health monitoring," *Smart Mater. Struct.* **13**, 415–423 (2004).
- ²⁵Ajit Mal, Fabrizio Ricci, Sauvik Banerjee, and Frank Shih, "A conceptual structural health monitoring system based on vibration and wave propagation," *Structural Health Monitoring: An International Journal* **4**(3), 283–293 (2005).